The $\Xi(1620)$ and $\Xi(1690)$ molecular states from $S = -2$ meson-baryon interaction up to next-to-leading order

A. Feijoo [a,*], V. Valcarce Cadenas [b], V.K. Magas [b,c]

[a] *Departamento de Física Teórica and IFIC, Centro Mixto Universidad de Valencia-CSIC, Institutos de Investigación de Paterna, Aptdo. 22085, 46071 Valencia, Spain*
[b] *Departament de Física Quàntica i Astrofísica, Universitat de Barcelona, Martí Franquès 1, 08028 Barcelona, Spain*
[c] *Institut de Ciències del Cosmos, Universitat de Barcelona, Martí Franquès 1, 08028 Barcelona, Spain*

A B S T R A C T

We have studied the meson-baryon interaction in the neutral $S = -2$ sector using an extended Unitarized Chiral Perturbation Theory, which takes into account not only the leading Weinberg-Tomozawa term (as all the previous studies in $S = -2$ sector), but also the Born terms and next-to-leading order contribution. Based on the SU(3) symmetry of the chiral Lagrangian we took most of the model parameters from the BCN model [1], where these were fitted to a large amount of experimental data in the neutral $S = -1$ sector. We have shown that our approach is able to generate dynamically both $\Xi(1620)$ and $\Xi(1690)$ states in very reasonable agreement with the data, and can naturally explain the puzzle with the decay branching ratios of $\Xi(1690)$. Our results clearly illustrate the reliability of chiral models implementing unitarization in coupled channels and the importance of considering Born and NLO contributions for precise calculations.

1. Introduction

The recent analysis of the $\Xi_b^- \to J/\psi \Lambda K^-$ decay by the LHCb Collaboration showed the presence of two narrow excited Ξ^- states in the $K^- \Lambda$ invariant mass distribution [2]. On a one to one assignation, the peak located at lower energy was identified as the $\Xi(1690)^-$ while the second one as the $\Xi(1820)^-$. Their masses and widths were measured with improved precision in comparison with [3], where the typical uncertainties are about 5 MeV. The corresponding data treatment and fitting procedure established the $\Xi(1690)^-$ mass and width as:

$$M = 1692.0 \pm 1.3^{+1.2}_{-0.4} \text{ MeV}, \ \Gamma = 25.9 \pm 9.5^{+14.0}_{-13.5} \text{ MeV}. \tag{1}$$

The LHCb measurement was preceded by the first observation of the $\Xi(1620)^0$ baryon decaying into $\Xi^- \pi^+$ via the $\Xi_c^+ \to \pi^+ \pi^+ \Xi^-$ process, which was collected with the Belle detector at the KEKB asymmetric-energy $e^+ e^-$ collider [4]. The subsequent data analysis determined its mass and width as:

$$M = 1610.4 \pm 6.0^{+6.1}_{-4.2} \text{ MeV}, \ \Gamma = 59.9 \pm 4.8^{+2.8}_{-7.1} \text{ MeV}. \tag{2}$$

In addition, the $\Xi^- \pi^+$ invariant mass distribution studied in [4] shed some more light on the structure of hyperon resonances with strangeness $S = -2$ by providing a clear signal of the $\Xi(1530)^0$ resonance and a structure that can be attributed to the $\Xi(1690)^0$ state.

With all previous measurements, and bearing in mind that the information reported by LHCb in [2] has not been yet updated in the PDG compilation [3], the $\Xi(1620)$ state is rated with a single star status and its spin and parity (J^P) need to be confirmed. Actually, it has been common practice to assume $J^P = 1/2^-$ as the corresponding spin-parity given the analogy with the $\Lambda(1405)$ as its counterpart in $S = -1$. Apparently, the status of the $\Xi(1690)^0$ seems to be clearer since it is rated with three-star and its spin-parity is established as $J^P = 1/2^-$ from an experimental evidence in the $\Lambda_c^+ \to K^+ \pi^+ \Xi^-$ decay [5].

On the theoretical side, there is still a long-term controversy about the nature of the $\Xi(1620)$ and $\Xi(1690)$ states. There are certain indications pointing to the fact that these states may have a nontrivial internal structure rather than a plain qqq configuration. On the one hand, as already mentioned, the unavoidable analogy between $\Xi(1620)$ and $\Lambda(1405)$ leads one to interpret the $\Xi(1620)$ as a molecular state arising from the Unitarized Chiral Perturbation (UChPT) scheme [3,6]. On the other hand, according to the study of [5], the spin-parity of the $\Xi(1690)$ should be $J^P = 1/2^-$, a fact that qualifies such a state to decay into the $\pi \Xi$, $\bar{K} \Lambda$ or $\bar{K} \Sigma$
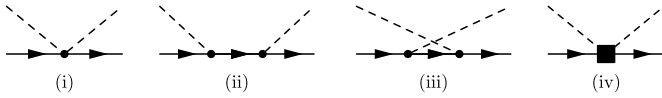
Fig. 1. Feynman diagrams for meson-baryon interaction: WT term (i), direct and crossed Born terms (ii) and (iii), and NLO terms (iv). Dashed (solid) lines represent the pseudoscalar octet mesons (octet baryons).

channels in s-wave. By inspecting the $\Xi(1690)$ branching ratios in [3], one can appreciate that the $\Gamma_{\pi\Xi}/\Gamma_{\bar{K}\Sigma}$ one is less than 0.09 in spite of the fact that $\pi\Xi$ has a much larger phase space than $\bar{K}\Sigma$. This issue was already addressed in [7], where the $\Xi(1690)$ was interpreted as a $\bar{K}\Sigma$ quasibound state dynamically generated from the Chiral Unitary approach in coupled channels [8,9]. The explanation for the smallness of the above branching ratio was found to be due to the nearly vanishing $\pi\Xi$ couplings.

Being chronologically accurate, the $S = -2$ meson-baryon interaction within the SU(3) UChPT approach in coupled channels was first employed in [10], the authors of which found one resonance that was assigned to the $\Xi(1620)$ state ruling out any possibility of being the $\Xi(1690)$ state. This work was followed by a similar study [11], and some of the previous authors revisited the meson-baryon interaction in $S = 0, -1, -2, -3$ sectors yet using a SU(6) extension of the Chiral Lagrangian within a coupled channel unitary approach in [12]. Among the large number of resonances found in these two last studies, the Ξ^* poles with $J^P = 1/2^-$ describe qualitatively the properties of the $\Xi(1620)$, $\Xi(1690)$ and $\Xi(1950)$ states. In [7], the $\Xi(1690)$ was dynamically generated in good agreement with experimental mass yet with a tiny width. Regarding the $\Xi(1620)$ state, only one virtual state was found at an energy more than 50 MeV below the experimental location. Recently, a new study [13] based on the same approach as the one in [10] pinned the $\Xi(1620)$ down to the experimental value at the expense of reducing unnaturally one of the parameters present in the unitarization method.

The forthcoming experiments studying hadronic decays of charm baryons, governed by $c \to s$ transitions, will provide more information about the $S = -2$ baryon spectroscopy. The ongoing measurements of $\gamma p \to K^+(\Lambda^*/\Sigma^*) \to K^+ K^{+/0}\Xi^{*-/0}(\to K^+ K^{+/0}\bar{K}\Lambda)$ by GlueX Collaboration [14] can also play a crucial role on this issue. Furthermore, the $K^-\Lambda$ Correlation Function can be experimentally accessed with Femptoscopy Technique by ALICE at LHC [15] as it was done for $\bar{K}N$ [16,17].

In view of that, the current theoretical models should be revisited and improved. In this sense, in the present work, we make a step forward and, for the first time in this sector, we take into account higher order contributions in the Lagrangian from which the interaction kernel is derived. In all previous theoretical works [7–13], only a contact Weinberg-Tomozawa (WT)-like term was used as interaction. Further perturbative corrections have been systematically ignored since they are assumed to play a very moderate role, specially, in s-wave. And, so far, it has been seen that these models provide a plausible explanation on the nature of these Ξ^* states in terms of meson-baryon molecules. However, we wonder how strong this assumption is and whether these higher order terms can help to describe accurately the mass and width of such states simultaneously, what was not achieved in the above cited papers.

In the $S = -1$ sector by looking at $\bar{K}N$ interaction we can find evidences of the non-negligible role of the s- and u-channels, known as direct and cross Born terms, and the tree level next-to-leading order (NLO) contribution, schematically shown in Fig. 1. For instance, in [18], the authors pointed out that the Born contributions reach 20% of the dominant WT contribution just 65 MeV above the $\bar{K}N$ threshold. As the energy increases moderately, the combined effect between the Born and the NLO terms plays a crucial role in the reproduction of the total cross section from

$\bar{K}N \to \eta\Lambda, \eta\Sigma, K\Xi$ processes [19,20,1]. At this point, it should be recalled that the value of the η-channel thresholds is located a little bit more than 200 MeV above $\bar{K}N$ threshold. Similarly, the difference between $\bar{K}^0\Lambda$ and the $\eta\Xi^0$ threshold is around 250 MeV. Thus, in the $S = -2$ sector a similar impact of these terms can be expected in the energy regime delimited by the higher thresholds. These new pieces in the interaction kernel will enable processes that are not connected with the WT term and, consequently, the additional interplay among the channels may affect the widths and the locations of the dynamically generated states.

With all this in mind, in the present study we have incorporated to the meson-baryon interaction in the neutral $S = -2$ sector, in addition to WT term, the s-, u-channel Born diagrams and the tree level NLO contribution, by adapting the BCN model (WT+Born+NLO model in [1]). And we show that such an extended model is able to generate dynamically both $\Xi(1620)$ and $\Xi(1690)$ states in a fair agreement with experimental data.

2. Formalism

The derivation of the meson-baryon interaction from effective chiral lagrangians has been addressed many times in literature [8,9,21]. Precisely for this reason, in this section we only highlight the main steps and underline the particularities of our model. As a starting point, the $SU(3)$ chiral effective Lagrangian up to NLO is taken into consideration, $\mathcal{L}_{\phi B}^{eff} = \mathcal{L}_{\phi B}^{(1)} + \mathcal{L}_{\phi B}^{(2)}$, with $\mathcal{L}_{\phi B}^{(1)}$ and $\mathcal{L}_{\phi B}^{(2)}$ being the most general form of the leading order and NLO contributions to meson-baryon interaction Lagrangian, respectively, defined as

$$\mathcal{L}_{\phi B}^{(1)} = i\langle \bar{B}\gamma_\mu[D^\mu, B]\rangle - M_0\langle\bar{B}B\rangle - \frac{1}{2}D\langle\bar{B}\gamma_\mu\gamma_5\{u^\mu, B\}\rangle$$
$$- \frac{1}{2}F\langle\bar{B}\gamma_\mu\gamma_5[u^\mu, B]\rangle , \qquad (3)$$

$$\mathcal{L}_{\phi B}^{(2)} = b_D\langle\bar{B}\{\chi_+, B\}\rangle + b_F\langle\bar{B}[\chi_+, B]\rangle + b_0\langle\bar{B}B\rangle\langle\chi_+\rangle$$
$$+ d_1\langle\bar{B}\{u_\mu, [u^\mu, B]\}\rangle + d_2\langle\bar{B}[u_\mu, [u^\mu, B]]\rangle$$
$$+ d_3\langle\bar{B}u_\mu\rangle\langle u^\mu B\rangle + d_4\langle\bar{B}B\rangle\langle u^\mu u_\mu\rangle . \qquad (4)$$

The 3×3 unitary matrix B contains the fundamental baryon octet (N, Λ, Σ, Ξ), in both equations. The incorporation of the pseudoscalar meson octet (π, K, η) requires a more complicated prescription, $u_\mu = iu^\dagger\partial_\mu Uu^\dagger$, to preserve the chiral symmetry. The pseudoscalar fields are collected in a 3×3 unitary ϕ matrix, which enters via $U(\phi) = u^2(\phi) = \exp\left(\sqrt{2}i\phi/f\right)$, where f is the meson decay constant. In Eqs. (3) and (4), the symbol $\langle\ldots\rangle$ stands for trace in flavor space.

The Low Energy Constants (LECs) D and F present in Eq. (3) are the so called $SU(3)$ axial vector constants, which are subjected to the constraint $g_A = D + F = 1.26$. In the same expression, M_0 is the common baryon octet mass in the chiral limit. The covariant derivative, $[D_\mu, B] = \partial_\mu B + [\Gamma_\mu, B]$ with $\Gamma_\mu = [u^\dagger, \partial_\mu u]/2$ being the chiral connection, is present in Eq. (3). Furthermore, in Eq. (4), we find $\chi_+ = 2B_0(u^\dagger\mathcal{M}u^\dagger + u\mathcal{M}u)$, which breaks chiral symmetry explicitly via the quark mass matrix $\mathcal{M} = \text{diag}(m_u, m_d, m_s)$ and $B_0 = -\langle 0|\bar{q}q|0\rangle/f^2$; the latter is related to the order parameter of spontaneously broken chiral symmetry. The corresponding LECs at NLO, namely b_D, b_F, b_0 and d_i ($i = 1, \ldots, 4$), need to be determined from experiment since they are not fixed by the symmetries of the underlying theory. Given the lack of scattering data availability in the $S = -2$ sector, we effectively assume the $SU(3)$ symmetry in the present work, and thus we use the LECs obtained in the $S = -1$ sector for the WT+Born+NLO model (see Table (II) in [1]).

Table 1
D_{ij} and L_{ij} coefficients in the NLO potential of the pseudoscalar meson and the baryon octet with strangeness $S = -2$ and charge $Q = 0$. The coefficients are symmetric, $D_{ji} = D_{ij}$ and $L_{ji} = L_{ij}$. With the definitions: $\mu_1^2 = m_K^2 + m_\pi^2$, $\mu_2^2 = 5m_K^2 - 3m_\pi^2$, $\mu_3^2 = 4m_K^2 - m_\pi^2$, $\mu_4^2 = 8m_K^2 - 3m_\pi^2$, $\mu_5^2 = 8m_K^2 - 5m_\pi^2$.

D_{ij}	$\pi^+\Xi^-$	$\pi^0\Xi^0$	$\bar{K}^0\Lambda$	$K^-\Sigma^+$	$\bar{K}^0\Sigma^0$	$\eta\Xi^0$
$\pi^+\Xi^-$	$2(2b_0+b_D-b_F)m_\pi^2$	0	$-(b_D-3b_F)\mu_1^2/\sqrt{6}$	0	$(b_D+b_F)\mu_1^2/\sqrt{2}$	$2\sqrt{2}(b_D-b_F)m_\pi^2/\sqrt{3}$
$\pi^0\Xi^0$		$4(b_0+b_D-b_F)m_\pi^2$	$(b_D-3b_F)\mu_1^2/2\sqrt{3}$	$(b_D+b_F)\mu_1^2/\sqrt{2}$	$(b_D+b_F)\mu_1^2/2$	$-2(b_D-b_F)m_\pi^2/\sqrt{3}$
$\bar{K}^0\Lambda$			$2(6b_0+5b_D)m_K^2/3$	$2\sqrt{2}b_D m_K^2/\sqrt{3}$	$-2b_D m_K^2/\sqrt{3}$	$(b_D-3b_F)\mu_2^2/6$
$K^-\Sigma^+$				$2(2b_0+b_D+b_F)m_K^2$	$-2\sqrt{2}b_F m_K^2$	$-(b_D+b_F)\mu_2^2/\sqrt{6}$
$\bar{K}^0\Sigma^0$					$2(2b_0+b_D)m_K^2$	$(b_D+b_F)\mu_2^2/2\sqrt{3}$
$\eta\Xi^0$						$2(2b_0\mu_3^2+b_D\mu_4^2+b_F\mu_5^2)/3$

L_{ij}	$\pi^+\Xi^-$	$\pi^0\Xi^0$	$\bar{K}^0\Lambda$	$K^-\Sigma^+$	$\bar{K}^0\Sigma^0$	$\eta\Xi^0$
$\pi^+\Xi^-$	$-d_1+d_2+2d_4$	0	$\sqrt{3}(d_1-d_2)/\sqrt{2}$	$-2d_2+d_3$	$(d_1+3d_2)/\sqrt{2}$	$-\sqrt{2}(d_1-3d_2)/\sqrt{3}$
$\pi^0\Xi^0$		$-d_1+d_2+2d_4$	$-(d_1-3d_2)/2\sqrt{3}$	$(d_1+d_2)/\sqrt{2}$	$-(d_1+d_2)/2$	0
$\bar{K}^0\Lambda$			$(d_1+3d_2+2d_4)/2$	$\sqrt{6}d_2$	$-\sqrt{3}d_2$	0
$K^-\Sigma^+$				0	$-\sqrt{2}d_1$	$-(d_1+3d_2)/\sqrt{6}$
$\bar{K}^0\Sigma^0$					d_2+2d_4	$(d_1+3d_2)/2\sqrt{3}$
$\eta\Xi^0$						$d_1+3d_2+2d_4$

In Fig. 1, the different contributions to the meson-baryon interaction kernel are diagrammatically represented. More precisely, the contact diagram (i) corresponds to the WT contribution; this comes from the term with the covariant derivative in Eq. (3). Next, the vertices of diagrams (ii) and (iii), which stand for the direct and crossed Born contributions, are obtained from the second and third terms of Eq. (3). And finally, the contribution of the NLO contact diagram, i.e. the fourth diagram of Fig. 1, is directly extracted from Eq. (4).

Thus, the total interaction kernel up to NLO can be expressed as the sum of all those terms: $V_{ij} = V_{ij}^{WT} + V_{ij}^{direct} + V_{ij}^{crossed} + V_{ij}^{NLO}$, where the elements of the $V_{ij} = \langle i|V|j \rangle$ interaction matrix couple the meson-baryon channels which, in the present case, amount to six: $\pi^0\Xi^0$, $\pi^+\Xi^-$, $\bar{K}^0\Lambda$, $K^-\Sigma^+$, $\bar{K}^0\Sigma^0$ and $\eta\Xi^0$. The explicit expressions for each contribution to the interaction kernel (for $S = -1$ sector) can be found in Eqs. (7)-(10) of [22] that, once projected onto s-wave, they recover the structure showed by Eqs. (6)-(8) and (10) in [20]. The expressions for $S = -2$ are just the same, but obviously the corresponding coefficients should be recalculated for this sector. Actually, the C_{ij} coefficients of the WT contact potential can be found in Table 1 of Ref. [7]. The baryon-meson-baryon coefficients present in the pseudoscalar-coupling vertexes in both Born diagrams can be obtained taking into account the relations (A.5) in Appendix A of Ref. [23]. Finally, one can find the NLO Clebsch-Gordan type coefficients, D_{ij} and L_{ij} in Eq. (10) of [20], displayed in Table 1.

Once the V_{ij} potential is calculated, the scattering matrix is obtained by solving the Bethe-Salpeter (BS) equation in coupled channels by factorizing the interaction kernel and the scattering amplitude out of the integral equation, leaving a simple system of algebraic equations to be solved which, in matrix form, reads as (see [1] and the references therein for a more detailed explanation) $T_{ij} = (1 - V_{il}G_l)^{-1}V_{lj}$, where T_{ij} represents the scattering amplitude for a given starting i-channel and an outgoing j-channel, and G_l is the loop function standing for a diagonal matrix with elements:

$$G_l = i \int \frac{d^4 q_l}{(2\pi)^4} \frac{2M_l}{(P-q_l)^2 - M_l^2 + i\epsilon} \frac{1}{q_l^2 - m_l^2 + i\epsilon}, \quad (5)$$

where M_l and m_l are the baryon and meson masses of the l-channel. The dimensional regularization is applied on this function because of its logarithmic divergence to finally get:

$$G_l = \frac{2M_l}{(4\pi)^2} \left\{ a_l(\mu) + \ln \frac{M_l^2}{\mu^2} + \frac{m_l^2 - M_l^2 + s}{2s} \ln \frac{m_l^2}{M_l^2} + \frac{q_{cm}}{\sqrt{s}} \ln \left[\frac{(s + 2\sqrt{s}q_{cm})^2 - (M_l^2 - m_l^2)^2}{(s - 2\sqrt{s}q_{cm})^2 - (M_l^2 - m_l^2)^2} \right] \right\}. \quad (6)$$

The loop function G_l comes in terms of the subtraction constants (SC) a_l that replace the divergence for a given dimensional regularization scale μ, which is taken to be 630 MeV in the present work. These constants are unknown, however, one can establish a natural size for them following [18], and it comes out to be around -2.0; in our study we will allow the substracting constants to vary within the interval $[-3.5, -1]$. In addition, isospin symmetry arguments are frequently used to reduce the number of independent SC, in particular, we consider 4 such constants here ($a_{\pi\Xi}$, $a_{\bar{K}\Lambda}$, $a_{\bar{K}\Sigma}$ and $a_{\eta\Xi}$).

The dynamically generated resonance states show up as pole singularities of the scattering amplitude at $\sqrt{s} = z_p = M_R - i\Gamma_R/2$, whose real and imaginary parts correspond to its mass (M_R) and the half width ($\Gamma_R/2$). The complex coupling strengths (g_i, g_j) of the resonance to the corresponding meson-baryon channels can be evaluated assuming a Breit-Wigner structure for the scattering amplitude in the proximity of the found pole on the real axis, $T_{ij}(\sqrt{s}) \sim g_i g_j/(\sqrt{s} - z_p)$.

3. Results

Our starting point is a model derived from a chiral Lagrangian up to NLO in s-wave (WT+Born+NLO model of [1]), which involves a number of parameters, LECs plus SC, that amount to a maximum of 16 in the $S = -1$ sector. In the sector of interest, $S = -2(Q = 0)$, due to a smaller number of available channels a number of parameters is reduced to 14, namely: the meson decay constant f, the axial vector couplings D and F, the NLO coefficients b_0, b_D, b_F, d_1, d_2, d_3, d_4; and four SC $a_{\pi\Xi}$, $a_{\bar{K}\Lambda}$, $a_{\bar{K}\Sigma}$ and $a_{\eta\Xi}$. In the present work, as first step, all the LECs are assumed to be $SU(3)$ symmetric, meaning that the values of f, D, F, b_0, b_D,

Table 2
Values of the parameters for the different models described in the text. The subtraction constants are taken at a regularization scale $\mu = 630$ MeV.

	Model I	Model II
$a_{\pi\Xi}$	-2.7981	-2.7228
$a_{\bar{K}\Lambda}$	-1.0071	-1.0000
$a_{\bar{K}\Sigma}$	-3.0938	-2.9381
$a_{\eta\Xi}$	-3.2665	-3.3984
f/f_π	1.196 (fixed [1])	1.204

b_F, d_1, d_2, d_3 and d_4 are fixed to the ones obtained in [1]. Thus, the strategy followed consists of varying the SC within a reasonable natural size range, $[-3.5, -1]$, in order to describe the masses and widths of the $\Xi(1620)$ and $\Xi(1690)$ states in the best possible way. This procedure is called Model I in the present study.

It is worth mentioning that, prior to proceed with the full interaction kernel, we take the leading order contact term (WT) as the only contribution in the interaction kernel and tried to reproduce the Ξ^* of interest by means of tuning the SC. As found in the literature mentioned above, one is able to dynamically generate two poles, but the features of those could not reproduce the experimental masses and widths of $\Xi(1620)$ and $\Xi(1690)$ at the same time. First of all, for WT-based models even if two resonances are generated there exists a mutual incompatibility in pinning both masses down simultaneously. Furthermore, the width of the $\Xi(1690)$ remains invariably small around 1 MeV. The $\Xi(1620)$ resonance can be reproduced very well, but only allowing some of the SC to take unnatural-size values.

By contrary, the situation rather improves when all contributions are included in the kernel. This is clearly seen by inspecting the results for Model I in Table 3 using the corresponding parametrization from Table 2. The most eye-catching output is the closeness of both masses to the experimental values simultaneously. In particular, the energy location of the pole associated to $\Xi(1620)$ is within the experimental error band (Eq. (2)) while the pole related to $\Xi(1690)$ is about 7 MeV below the lower edge of the corresponding experimental error band (Eq. (1)). Furthermore, the value for the theoretical width of $\Xi(1690)$ is within the error band (Eq. (1)). This is in contrast to what happens to the theoretical $\Xi(1620)$ width that reaches about a factor 2.5 bigger than the nominal value (Eq. (2)) (this issue is addressed below).

As a next step, in Model II we decided to consider the global scaling factor f as a free parameter of the model, yet keeping it constrained within the corresponding error bands of the BCN model (Table II of Ref. [1]). Actually, the value of the constant f in our model does not correspond exactly to the known experimental value of f_π, because it effectively takes into account the role of kaons and η's in the system. This is a general feature of the studies were UChPT models are fitted to the data - effectively f is a bit larger than f_π. However, the role of each pseudoscalar meson in the $S = -2$ sector differs from the one in the $S = -1$ sector, studied in [1], therefore it is reasonable to readjust the f value for the current study.

As it could be expected, because of the increased relative relevance of $\bar{K}$'s and η's over π's in the $S = -2$ sector, our system prefers a bit higher value for f (see results for Model II in Table 2). On the other hand, the corresponding SC barely differ from those of Model I. These combined modifications provide however a notable improvement of the pole location in the complex plane in order to describe the experimental states as seen in Table 3. The theoretical masses reach values closer to the nominal ones, the same can be said about the theoretical $\Xi(1690)$ width. Regarding the $\Xi(1620)$ width for Model II, the new value exceeds by 10 MeV that of Model I.

Table 3
Comparison of the pole positions between the models: Model I and Model II (in MeV) with their couplings g_i and the corresponding modulus found in $J^P = \frac{1}{2}^-$, $(I, S) = (\frac{1}{2}, -2)$.

Model I	$\Xi(1620)$		$\Xi(1690)$	
M [MeV]	1599.95		1683.04	
Γ [MeV]	158.88		11.51	
	g_i	$|g_i|$	g_i	$|g_i|$
$\pi^+\Xi^-$	$1.70 + i0.78$	1.87	$0.44 + i0.07$	0.45
$\pi^0\Xi^0$	$-1.22 - i0.62$	1.37	$0.08 - i0.10$	0.13
$\bar{K}^0\Lambda$	$-2.11 - i0.08$	2.11	$0.50 - i0.06$	0.51
$K^-\Sigma^+$	$0.81 - i0.22$	0.84	$1.0 - i0.16$	1.01
$\bar{K}^0\Sigma^0$	$-0.41 + i0.28$	0.50	$-1.34 + i0.26$	1.37
$\eta\Xi^0$	$-0.23 + i0.13$	0.26	$-0.74 + i0.13$	0.76

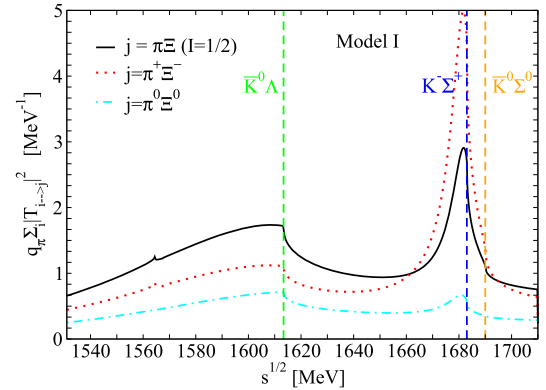| Model II	$\Xi(1620)$		$\Xi(1690)$	
M [MeV]	1608.51		1686.17	
Γ [MeV]	170.00		29.72	
	g_i	$|g_i|$	g_i	$|g_i|$
$\pi^+\Xi^-$	$1.73 + i0.85$	1.93	$0.51 + i0.25$	0.57
$\pi^0\Xi^0$	$-1.24 - i0.67$	1.41	$0.09 - i0.06$	0.11
$\bar{K}^0\Lambda$	$-2.12 - i0.09$	2.12	$0.81 - i0.02$	0.81
$K^-\Sigma^+$	$0.8 - i0.25$	0.84	$1.36 + i0.10$	1.36
$\bar{K}^0\Sigma^0$	$-0.36 + i0.31$	0.48	$-1.99 + i0.08$	1.99
$\eta\Xi^0$	$-0.20 + i0.12$	0.24	$-1.04 + i0.06$	1.04

Fig. 2. Sum of amplitudes squared times a phase space factor. The vertical dashed lines represent the channel threshold locations.

To aid the understanding of the apparent incompatibility between the theoretical and the experimental width of the $\Xi(1620)$ state and to give an idea of the $\pi\Xi$ spectrum that our models would provide, the quantity $q_\pi |\sum_i T_{i\to\pi\Xi}|^2$ is represented in Figs. 2 and 3, where $T_{i\to\pi\Xi}$ is the amplitude for the $i \to \pi\Xi$ transition obtained here with either Model I (Fig. 2) or Model II (Fig. 3), with i taking any of the six coupled channels involved in this sector and the final $\pi\Xi$ state can denote any of the physical channels: $\pi^+\Xi^-$, $\pi^0\Xi^0$. The momentum of the π meson in the $\pi\Xi$ center-of-mass frame, q_π, acts as a phase-space modulator. We note that, in front of each amplitude $T_{i\to\pi\Xi}$ in the former expression, one should have included a coefficient gauging the strength with which the production mechanism excites the particular meson-baryon channel i. Given the qualitative character of this production mechanism, we have assumed all these coefficients to be equal. Returning to the problem of the oversized theoretical $\Xi(1620)$ width, either Fig. 2 or Fig. 3 clearly show an effective reduction of the width compared to the theoretical value because of
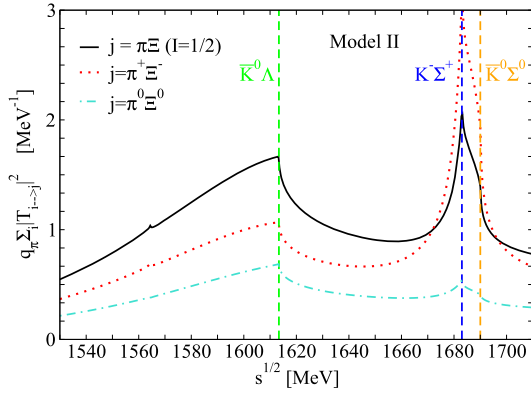
Fig. 3. Sum of amplitudes squared times a phase space factor. The vertical dashed lines represent the channel threshold locations.

Table 4
Effective range, r_{eff}, and scattering length, a_0, for $\bar{K}^0 \Lambda$ threshold.

	Model I	Model II
$a_0^{\bar{K}^0 \Lambda}$	$-0.155 + i\, 0.501$	$-0.115 + i\, 0.495$
$r_{eff}^{\bar{K}^0 \Lambda}$	$-0.408 - i\, 0.413$	$-0.507 - i\, 0.205$

the Flatté effect [24]. This is a well-known effect that takes place when a resonance is located below a threshold of a channel whose coupling to this structure is strong, and this is exactly the situation with the $\bar{K}^0 \Lambda$ which opens 5 MeV above the peak of the theoretical resonance. If we focus on the first structure generated by Model II, which we consider our best model, the width is around 90 MeV that it is in much better agreement with the measured one Eq. (2). The second structure present in Fig. 3 also shows a threshold effect produced by the opening of the $K^- \Sigma^+$ that distorts the typical Breit-Wigner shape of a resonance. In any case, and despite being merely indicative and lacking of any background by construction, the spectra displayed in both Figures reproduces qualitatively well the structures present in the experimental $\pi^+ \Xi^-$ spectrum shown in FIG. 2 of [4].

For a general 2-body decay, the total width of a s-wave resonance with mass M_R into the ith-channel is proportional to $\Gamma_R^i \sim p_i |g_{R,i}|^2 M_i / M_R$, [25] where the p_i is the modulus of the outgoing-particle three-momentum in the parent's rest frame, and $g_{R,i}$ stands for the coupling of the resonance to the corresponding ith-channel. If a threshold position is in the vicinity of a resonance, as in the case of the $\bar{K} \Sigma$ thresholds to the $\Xi(1690)$ resonance (see Fig. 3), the effect of the finite width of the resonance on the corresponding partial decay width should be considered by convoluting the spectral function of the resonance, see Eq. (17) in Ref. [25]. Now, using the corresponding coupling from Table 3, we can compute the $\Xi(1690)$ branching ratios for our best model, Model II.

$$B_1 = \frac{\Gamma_{\Xi(1690)}^{\pi \Xi}}{\Gamma_{\Xi(1690)}^{\bar{K} \Sigma}} = \frac{\Gamma_{\Xi(1690)}^{\pi^+ \Xi^-} + \Gamma_{\Xi(1690)}^{\pi^0 \Xi^0}}{\Gamma_{\Xi(1690)}^{K^- \Sigma^+} + \Gamma_{\Xi(1690)}^{\bar{K}^0 \Sigma^0}} = 0.25 \,,$$

$$B_2 = \frac{\Gamma_{\Xi(1690)}^{\bar{K} \Sigma}}{\Gamma_{\Xi(1690)}^{\bar{K} \Lambda}} = \frac{\Gamma_{\Xi(1690)}^{K^- \Sigma^+} + \Gamma_{\Xi(1690)}^{\bar{K}^0 \Sigma^0}}{\Gamma_{\Xi(1690)}^{\bar{K} \Lambda}} = 3.22 \,.$$

Comparing our theoretical values of B_1 and B_2 to the experimental ones [3] we can see that they are not only of the same order of magnitude but also, in the case of B_2, the branching ratio is within the range of the experimental values. Thus, we obtained a natural explanation for the $\Xi(1690)$ decay branching ratios even without including these data into a fitting procedure.

To complete presenting the results of our model, we also calculate the effective range and scattering length at $\bar{K}^0 \Lambda$ threshold and show these in Table 4. These values potentially can be extracted from the Correlation Function using femtoscopy techniques by ALICE collaboration, similarly to the ongoing analysis of the $K^- \Lambda$ ones [15].

4. Conclusions

We have studied the meson-baryon interaction in the neutral $S = -2$ sector within an extended UChPT scheme, in which we take into account not only the leading WT term, but also the Born terms and NLO contribution for the first time in this sector. Most of the model parameters have been assumed to be $SU(3)$ symmetric and taken from the BCN model [1], where these were fitted to the large amount of experimental data in the neutral $S = -1$ sector, while the SCs have been taken as a free fitting parameters within their natural size limits.

We have shown that our model is able to generate dynamically both $\Xi(1620)$ and $\Xi(1690)$ states in a very reasonable agreement with the known experimental data. It is also important that the molecular nature of these states, provided by the present approach, naturally explains the puzzle with the decay branching ratios of $\Xi(1690)$. Thus, once again, the reliability of the chiral models with unitarization in coupled channels and the importance of considering Born and NLO contributions for precise calculations have been proved.

Declaration of competing interest

The authors declare that they have no known competing financial interests or personal relationships that could have appeared to influence the work reported in this paper.

Data availability

No data was used for the research described in the article.

References

[1] A. Feijoo, V. Magas, A. Ramos, $S = -1$ meson-baryon interaction and the role of isospin filtering processes, Phys. Rev. C 99 (3) (2019) 035211, https://doi.org/10.1103/PhysRevC.99.035211, arXiv:1810.07600.

[2] R. Aaij, et al., Evidence of a $J/\psi\Lambda$ structure and observation of excited Ξ^- states in the $\Xi_b^- \to J/\psi\Lambda K^-$ decay, Sci. Bull. 66 (2021) 1278–1287, https://doi.org/10.1016/j.scib.2021.02.030, arXiv:2012.10380.

[3] R.L. Workman, et al., Rev. Part. Phys. 2022 (2022) 083C01, https://doi.org/10.1093/ptep/ptac097.

[4] M. Sumihama, et al., Observation of $\Xi(1620)^0$ and evidence for $\Xi(1690)^0$ in $\Xi_c^+ \to \Xi^-\pi^+\pi^+$ decays, Phys. Rev. Lett. 122 (7) (2019) 072501, https://doi.org/10.1103/PhysRevLett.122.072501, arXiv:1810.06181.

[5] B. Aubert, et al., Measurement of the Spin of the Xi (1530) Resonance, Phys. Rev. D 78 (2008) 034008, https://doi.org/10.1103/PhysRevD.78.034008, arXiv: 0803.1863.

[6] D. Jido, J.A. Oller, E. Oset, A. Ramos, U.G. Meissner, Chiral dynamics of the two Lambda(1405) states, Nucl. Phys. A 725 (2003) 181–200, https://doi.org/10.1016/S0375-9474(03)01598-7, arXiv:nucl-th/0303062.

[7] T. Sekihara, $\Xi(1690)$ as a $\bar{K}\Sigma$ molecular state, PTEP 2015 (9) (2015) 091D01, https://doi.org/10.1093/ptep/ptv129, arXiv:1505.02849.

[8] N. Kaiser, P.B. Siegel, W. Weise, Chiral dynamics and the low-energy kaon - nucleon interaction, Nucl. Phys. A 594 (1995) 325–345, https://doi.org/10.1016/0375-9474(95)00362-5, arXiv:nucl-th/9505043.

[9] E. Oset, A. Ramos, Nonperturbative chiral approach to s wave anti-K N interactions, Nucl. Phys. A 635 (1998) 99–120, https://doi.org/10.1016/S0375-9474(98)00170-5, arXiv:nucl-th/9711022.

[10] A. Ramos, E. Oset, C. Bennhold, On the spin, parity and nature of the Xi (1620) resonance, Phys. Rev. Lett. 89 (2002) 252001, https://doi.org/10.1103/PhysRevLett.89.252001, arXiv:nucl-th/0204044.

[11] C. Garcia-Recio, M.F.M. Lutz, J. Nieves, Quark mass dependence of s wave baryon resonances, Phys. Lett. B 582 (2004) 49–54, https://doi.org/10.1016/j.physletb.2003.11.073, arXiv:nucl-th/0305100.

[12] D. Gamermann, C. Garcia-Recio, J. Nieves, L.L. Salcedo, Odd Parity Light Baryon Resonances, Phys. Rev. D 84 (2011) 056017, https://doi.org/10.1103/PhysRevD.84.056017, arXiv:1104.2737.

[13] T. Nishibuchi, T. Hyodo, Nature of excited Ξ baryons with threshold effects, EPJ Web Conf. 271 (2022) 10002, https://doi.org/10.1051/epjconf/202227110002, arXiv:2208.14608.

[14] P. Pauli, The strangeness program at GlueX, EPJ Web Conf. 271 (2022) 02001, https://doi.org/10.1051/epjconf/202227102001, arXiv:2209.00360.

[15] S. Acharya, et al., ΛK femtoscopy in Pb-Pb collisions at $\sqrt{s_{NN}}$ = 2.76 TeV, Phys. Rev. C 103 (5) (2021) 055201, https://doi.org/10.1103/PhysRevC.103.055201, arXiv:2005.11124.

[16] S. Acharya, et al., Scattering studies with low-energy kaon-proton femtoscopy in proton-proton collisions at the LHC, Phys. Rev. Lett. 124 (9) (2020) 092301, https://doi.org/10.1103/PhysRevLett.124.092301, arXiv:1905.13470.

[17] Constraining the $\bar{K}N$ coupled channel dynamics using femtoscopic correlations at the LHC (5 2022) arXiv:2205.15176.

[18] J.A. Oller, U.G. Meissner, Chiral dynamics in the presence of bound states: Kaon nucleon interactions revisited, Phys. Lett. B 500 (2001) 263–272, https://doi.org/10.1016/S0370-2693(01)00078-8, arXiv:hep-ph/0011146.

[19] A. Feijoo, V.K. Magas, A. Ramos, The $\bar{K}N \to K\Xi$ reaction in coupled channel chiral models up to next-to-leading order, Phys. Rev. C 92 (1) (2015) 015206, https://doi.org/10.1103/PhysRevC.92.015206, arXiv:1502.07956.

[20] A. Ramos, A. Feijoo, V.K. Magas, The chiral S = −1 meson–baryon interaction with new constraints on the NLO contributions, Nucl. Phys. A 954 (2016) 58–74, https://doi.org/10.1016/j.nuclphysa.2016.05.006, arXiv:1605.03767.

[21] M.F.M. Lutz, E.E. Kolomeitsev, Relativistic chiral SU(3) symmetry, large N(c) sum rules and meson baryon scattering, Nucl. Phys. A 700 (2002) 193–308, https://doi.org/10.1016/S0375-9474(01)01312-4, arXiv:nucl-th/0105042.

[22] A. Feijoo, D. Gazda, V. Magas, A. Ramos, The KN Interaction in Higher Partial Waves, Symmetry 13 (8) (2021) 1434, https://doi.org/10.3390/sym13081434, arXiv:2107.10560.

[23] B. Borasoy, R. Nissler, W. Weise, Chiral dynamics of kaon-nucleon interactions, revisited, Eur. Phys. J. A 25 (2005) 79–96, https://doi.org/10.1140/epja/i2005-10079-1, arXiv:hep-ph/0505239.

[24] S.M. Flatte, Coupled - Channel Analysis of the pi eta and K anti-K Systems Near K anti-K Threshold, Phys. Lett. B 63 (1976) 224–227, https://doi.org/10.1016/0370-2693(76)90654-7.

[25] L.S. Geng, E. Oset, M. Doring, The Radiative decay of the Lambda(1405) and its two-pole structure, Eur. Phys. J. A 32 (2007) 201–211, https://doi.org/10.1140/epja/i2007-10371-0, arXiv:hep-ph/0702093.